The Climate of China and Global Climate

Proceedings of
the Beijing International Symposium on Climate
Oct. 30 – Nov. 3, 1984 Beijing, China

Edited by
Ye Duzheng, Fu Congbin,
Chao Jiping and M. Yoshino

(1987)

With 357 Figures

China Ocean Press Beijing
Springer-Verlag Berlin Heidelberg New York
London Paris Tokyo

Secular Fluctuations of Temperature over Northern Hemisphere Land Areas and Mainland China since the Mid-19th Century

R. S. Bradley[1], H. F. Diaz[2], P. D. Jones[3] and P. M. Kelly[3]

Abstract – A comprehensive set of long-term temperature station records from throughout the Northern Hemisphere has been used to produce a gridded data set for studies of long-term climatic variability. Areally weighted and normalised seasonal average temperatures for Northern Hemisphere land areas and for mainland China have been computed for 1851–1980 and 1881–1980, respectively. Both records show similar trends; temperature increased from the late 19th century to a maximum in the 1940s followed by a cooling trend which has reversed over the last 10–15 years. In the Northern Hemisphere record, temperatures appear to have decreased from the 1850s to the 1880s but the spatial coverage is poor during this period. Data from China are highly correlated with Northern Hemisphere land area data, suggesting that long-term proxy records from China will provide valuable indications of climatic fluctuations over a much larger area. Extremely sharp drops in temperature, particularly in Fall months, occurred after several major volcanic eruptions. High temperatures are sometimes associated with major El Nino years. On occasions, when an El Nino event has followed a large explosive eruption, the two opposing effects have tended to minimize the climatic fluctuation which would otherwise have resulted.

Introduction

The concentration of carbon dioxide in the atmosphere has increased ~26% since the middle of the last century (Stuiver 1978; Keeling *et al.* 1982). According to recent projections (Edmonds ° s al. 1984) by about the year 2060 the concentration may reach ~600 ppmv, more than double the level prior to the industrial revolution. In view of the important rôle that CO^2 plays in the global energy balance, concern has been expressed about the potential climatic effects this build-up may produce (MacCracken and Luther 1985). Two strategies have generally been followed to evaluate this question: (a) modelling and theoretical studies of future atmospheric conditions with enhanced CO^2 concentrations (e.g. Manabe and Wetherald 1980; Hansen *et al.* 1981) and (b) empirical studies of past climatic conditions to evluate if a "CO^2 signal" can be detected in the climatic record of the last 100–150 years (e.g. Wigley and Jones, 1981; Wigley, et al. 1985) and to assess the role of other factors which may have contributed to climatic variability over this period, and which may be important in the future (e.g. Mitchell 1983; Kelly and Sear 1984).

Here we describe the results of a study of long-term temperature records from land areas of the northern hemisphere. Analysis of long-term data may facilitate the detection of CO_2 effects by providing a better estimate of the range of

1. University of Massachusetts, Amherst, Ma., U.S.A.
2. NOAA/ERL, Boulder, Co., U.S.A.
3. Climatic Research Unit, University of East Anglia, Norwich, U.K.

tate the detection of CO^2 effects by providing a better estimate of the range of
natural climatic variability. Particular attention is paid to the instrumental record from China to assess whether long, proxy climatic records from this region may provide a surrogate measure of temperature fluctuations over a much larger area for the period prior to the start of instrumental records (cf. Jones and Kelly 1983).

Data and Methodology

After a careful search of data archives and early meteorological publications, a high quality set of long-term temperature records has been assembled and digitized (Bradley *et al.* 1985). In order to make these records comparable, and in order to avoid combining data which varies widely in absolute terms, all values were expressed as departures from a reference period to enable the maximum number of station records to be compared over the longest interval of time. The optimum period for this purpose was 1946–1960. Accordingly, each set of station data was converted thus:

$$x_{ij} = x_{ij} - x_i$$

were x_{ij} is the data value for month i, year j and x_i is the 1946–60 average for month i, at the same station. The resulting station anomaly data were then used to interpolate values at grid points spaced at 5° latitude and 10° longitude intervals. By gridding the data, those areas which have dense concentrations of stations are not over-represented in areal averages and the effects of any minor inhomogeneities and locally unrepresentative data are minimized. The interpolation procedure involved fitting an inverse distance least-squares, best fit plane to anomaly values at the six stations nearest the grid point (see Jones *et al.* 1982 for details). This procedure was repeated for all grid points, for all months from January 1851 to December 1980.

Grid coverage is limited to land areas and adjacent oceanic regions, and is not evenly distributed through time (Fig. 1). The maximum coverage occurred in the 1950s, for which period ~57% of the surface area of the Northern Hemisphere can be gridded. Only ~8% of the area of the hemisphere can be gridded for the 1850s, when data collection was restricted mainly to Europe and eastern North America. This change in spatial coverage through time is an important characteristic of the Northern Hemisphere long-term temperature data set and must be considered in any study of hemispheric or regional averages over time.

Temperature Fluctuations: Northern Hemisphere Land Areas

To examine trends in temperature over the last 130 years, gridded anomaly data were averaged by zonal bands (5°–25°N, 30°–55°N and 60°–85°N) and for the hemisphere as a whole (5°–85°N). Grid values were weighted by the cosine of latitude to produce spatially representative averages. Figure 2 shows the resulting values. Each value plotted is a seasonal average (Winter = December, January,

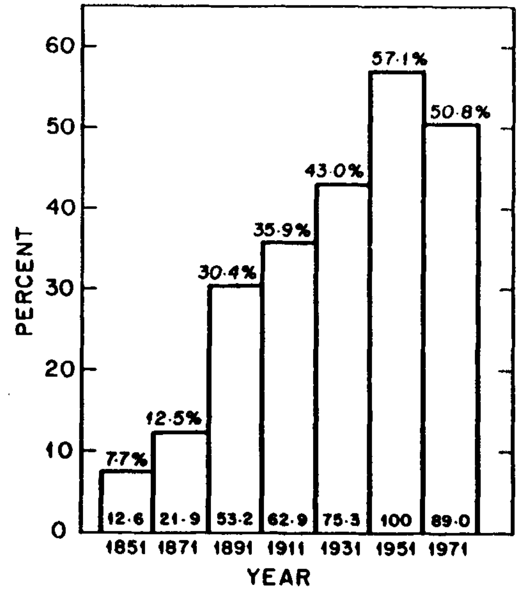

Fig. 1. Percentage of surface area of Northern Hemisphere "represented" by gridded land-based temperature data set, at 20 year intervals. Optimum coverage is in the 1950s when data are available for ~57% of the hemisphere. One hundred years carleer the area which can be gridded was only 7.7% of the surface area of the hemisphere (12.6% of the 1950s coverage)

February; Spring = March, April, May; Summer = June, July, August; Fall = September, October, November). Clearly seen are the generally lower temperatures of the 19th century (particularly the 1880s) and the marked warming episode from ~1915–1925 leading to maximum anomalies in the 1930s and 1940s, followed by declining temperature to the mid 1960s. Since 1965 a warming trend is evident. Of particular note is the pronounced increase in interannual variability from low to high latitudes (cf. Kelly *et al.* 1982). To take this into account, the data were next normalized by dividing each monthly grid-point anomaly value by the standard deviation of the grid point for the respective month in the 1946–60 reference period, viz:

$$x'_{ij} = \frac{x_{ij}}{\sigma_i}$$

where x_{ij} is the anomaly value for month i, year j at each grid point and σ_i is the standard deviation of month i in 1946–60 at the same location.

The resulting values (again weighted by the cosine of latitude) were then averaged to produce normalized, areally weighted hemispheric averages of seasonal temperature anomalies from the 1946–1960 reference period (Fig. 3). Seasonal data were also combined to produce a record of mean annual anomalies (Fig. 4).

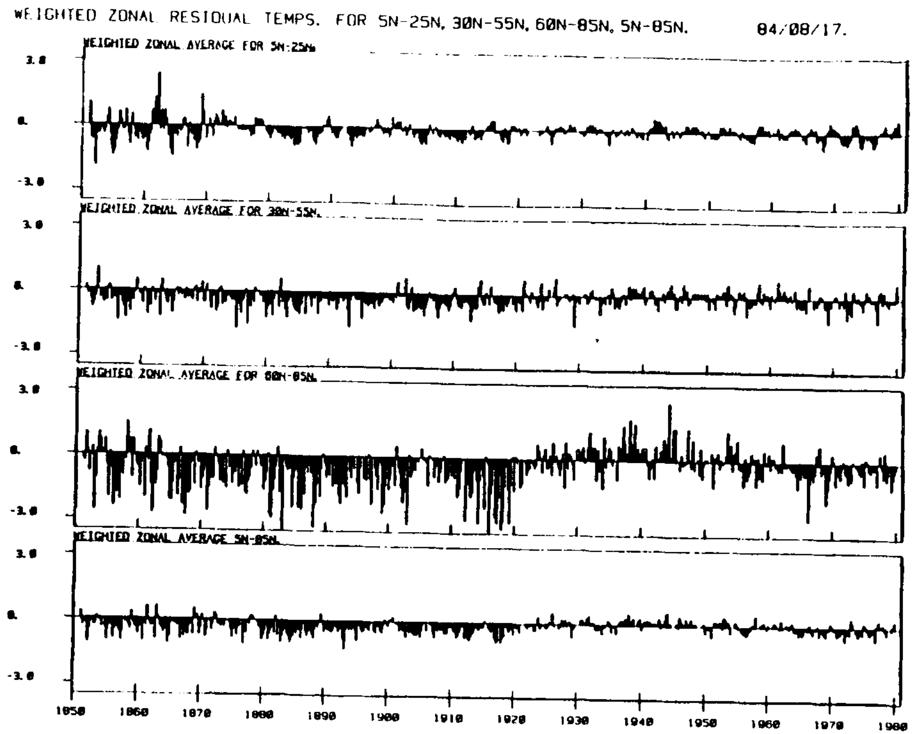

Fig. 2. Temperature anomalies (°C) from the reference period (1946–60) for three latitude bands and for the hemisphere as a whole (bottom). The difference in variability between different latitude bands is clearly seen. Values, plotted are 3-month (one season) averages, beginning with Spring (March, April, May) 1851

All seasons show the same basic low frequency characteristics; temperatures were steady, or increased from mid-1850s to the early 1870s, then fell, to reach minimum values in the 1880s. Temperatures increased to a maximum around 1940, mainly in two stages, from ~1880 to 1900 and from 1915 to 1930. After the 1940s peak, temperatures decreased to the early 1970s, followed by a slight increase in recent years. More recent data (not shown) indicate that this recent warming trend has continued into the early 1980s. In fact, the 5–year average (1980–1984) is the highest in the 130 year record (Kelly *et al.* 1985). Among the more important differences between the seasonal records, the relatively high temperature in summer months (and to some extent in Spring) during the late 1860s and 1870s is of interest. In summer months, temperatures at this time generally exceeded that of the reference period (1946–1960). However, it must be recognized that data coverage in the 1870s was only ~25% of that in the 1946–60 period (Fig. 1). Furthermore, differences in methods used to compute daily and monthly mean temperatures have changed over time (Bradley et al. 1985) so the two periods may not be directly comparable.

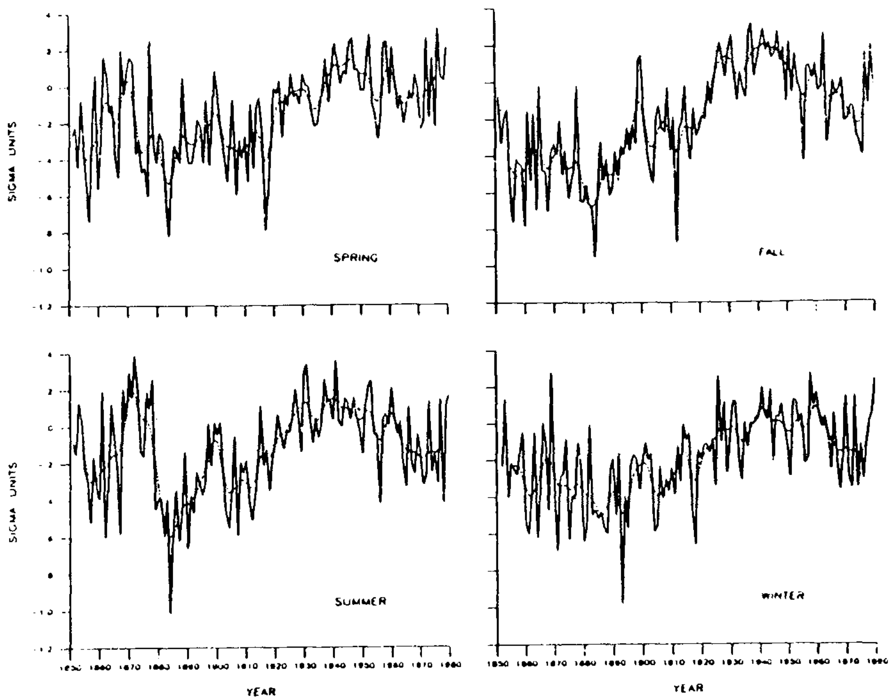

Fig. 3. Normalized, areally weighted seasonal temperature anomalies (from the 1946–1960 reference period) for Northern Hemisphere land areas. Spring = March, April, May; Summer = June, July, August; Fall = September, October, Norvember; Winter = December, January, February (value plotted for the year in which the December occurs, i.e. 1851/2 plotted as 1851). Dark line is a binomially weighted filter which smooths out high frequencies with a period of <10 years

Temperature Fluctuations in China

To investigate whether temperature fluctuations in China over the last 100 years were similar to those over Northern Hemisphere land areas as a whole, a subset of the hemispheric gridded data set was extracted for the area of mainland China (Fig. 5). The same computational procedure already described was carried out on the smaller "China grid" data set. However, unlike the Northern Hemisphere, the best data coverage for China is in the period 1961–1970. Consequently, all anomaly values in the China data set were normalized with respect to 1961–1970. The resulting areally weighted, normalized temperature anomaly graphs are shown in Figs. 6 and 7. Before 1881, there were insufficient data to permit a meaningful regional average to be computed for Mainland China.

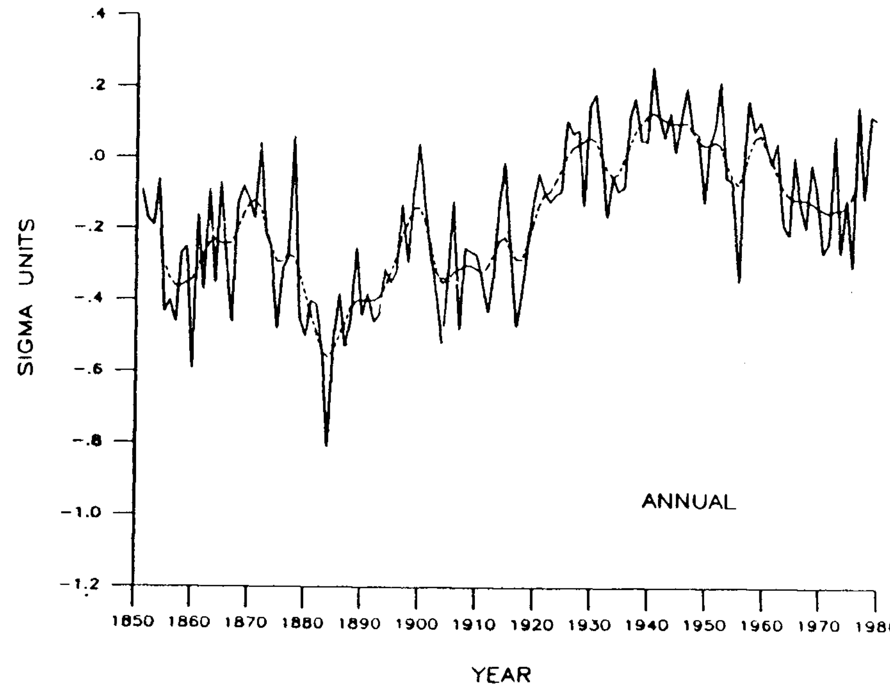

Fig. 4. Normalized areally weighted annual temperature anomalies (from 1946–60 reference period) for Northern Hemisphere land areas. Annual values produced from averaging seasonal values shown in Fig. 3

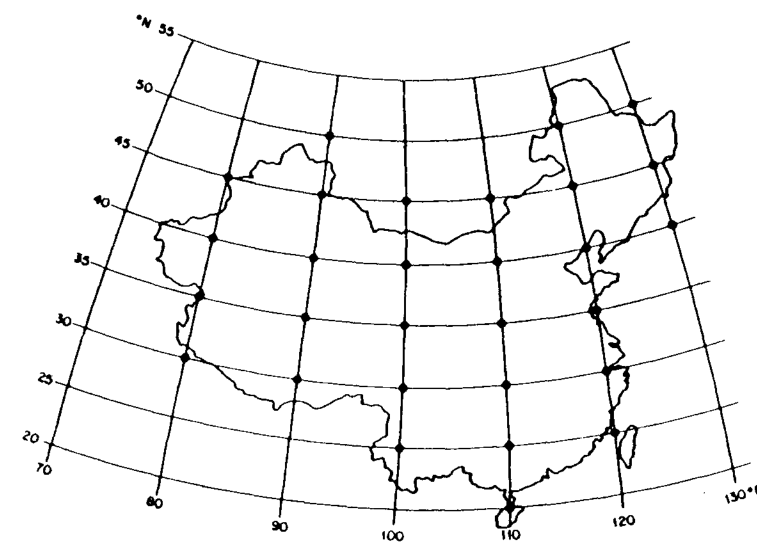

Fig. 5. Grid points (circled) selected for computation of temperature anomalies of China

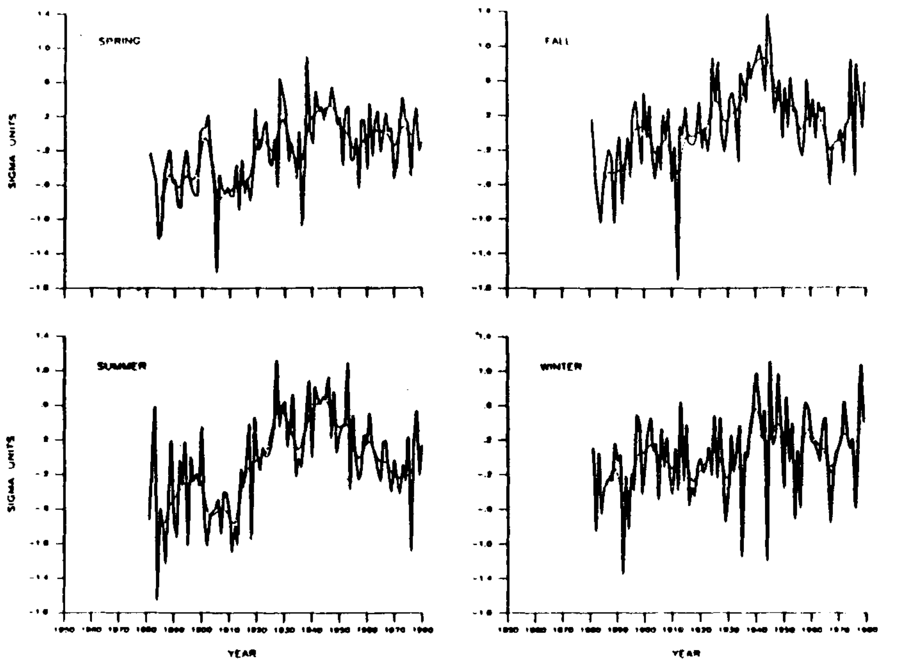

Fig. 6. Normalized areally weighted seasonal temperature anomalies (from the 1961–70 reference period) for China grid (shown in Fig. 5). Dark line is a binomially weighted filter which smooths out high frequencies with a period of <10 years

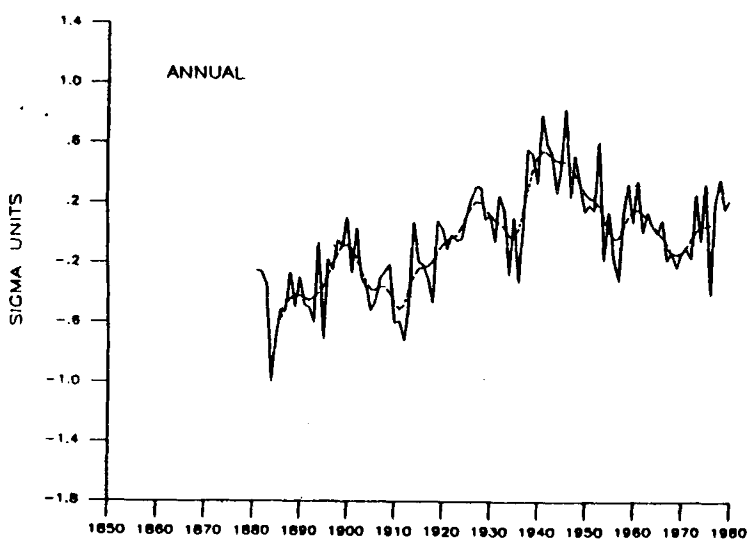

Fig. 7 Normalized, areally weighted annual temperature anomalies (from the 1961–70 reference period) for China grid (shown in Fig. 5)

The general trends (low frequency variations) were similar in China compared to the hemisphere land areas as a whole. However, the Chinese subset shows a more pronounced warming period in the late 1930s, particularly in Fall and Winter months (September–February). This is seen most clearly in Fig. 8 where the low frequency trends have been plotted for direct comparison with those of the Northern Hemisphere (Fig. 9). Both data sets indicate the warmest period of

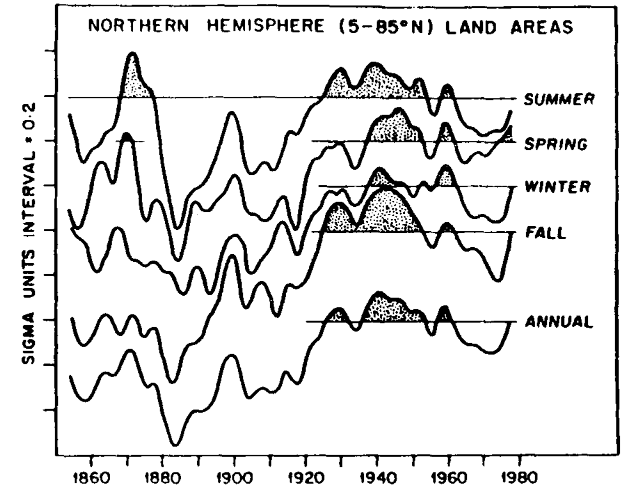

Fig. 8. Seasonal and annual low frequency temperature fluctuations of Northern Hemisphere land areas (from Figs. 3 and 4). The zero reference point has been displaced arbitrarily to enable trends to be compared. The same ordinate scale is used for each plot

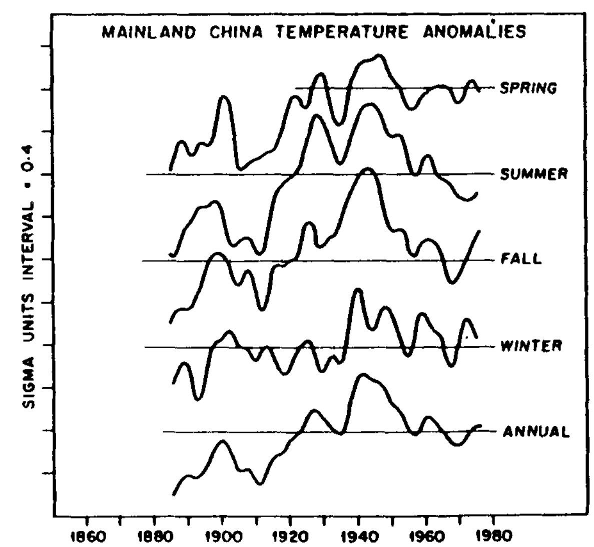

Fig. 9. Seasonal and annual low frequency temperature fluctuations of China (from Figs. 6 and 7). The zero reference point has been displaced arbitrarily to enable trends to be compared. The same ordinate scale has been used for each plot

the 20th century was the 1940s, followed by a cooling trend which seems to have reversed in the last decade or so. Although the Chinese data comprise a subset of the hemispheric land area data, they comprise a small fraction of the total number of data points, so the correlations are quite remarkable. Table 1 shows correlation coefficients between temperature anomalies for Northern Hemisphere land areas and China for the period 1881–1980. All coefficients are statistically significant (pH0.001). Correlation of the annual smoothed records (Fig. 10)

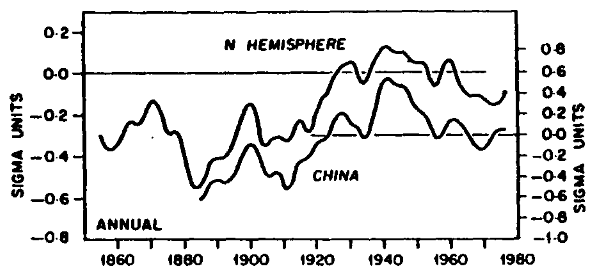

Fig. 10. Annual smoothed temperature anomalies for China and Northern Hemisphere land areas compared. Left scale is for Norhtern Hemisphere, right scale for China. Zero reference point has been displaced arbitrarily to permit comparison

Table 1. Correlation coefficients between areally weighted, normalised temperature anomalies of Northern Hemisphere land areas and mainland China, 1881–1980

Raw data											
J	F	M	A	M	J	J	A	S	O	N	D
0.46	0.52	0.55	0.55	0.40	0.58	0.54	0.53	0.55	0.45	0.52	0.41

	Spring	Summer	Fall	Winter	Annual
Raw Data	0.66	0.67	0.68	0.54	0.81
Smoothed Data [a]	0.92	0.93	0.90	0.68	0.95

a Binomially filtered; a 9-point weighting function was used with the following weights: 1, 5, 12, 20, 24, 20, 12, 5, 1

is exceptionally high. This suggests that China is a key area in studies of long-term climatic fluctuations. In particular, it seems likely that Chinese historical records of temperature (e.g. Zhang and Gong 1979; Zhang 1980) could be used as a proxy record of temperature fluctuations over Northern Hemisphere land

area as a whole, particularly for studies of low frequency trends.

High Frequency Climatic Fluctuations

Of particular interest in the Northern Hemisphere and China area seasonal temperature records are the "spikes" of unusually low and (to a lesser extent) high temperatures which can be seen in the inter-annual data (Figs. 3 and 6). It is significant that the extremely low temperatures which occur in Fall months generally coincide with major explosive volcanic eruptions (Simkin *et al.* 1981), the most important of which appear to have been Krakatau (1883), Katmai (1912) and Bezymianny in 1956 (Table 2). The major effect is short-lived and only occurs

Table 2. Major explosive volcanic eruptions (VEI ≥5), 1851 – 1980 (after Simkin, *et al.* 1981)

Name of Volcano	Location	Date of eruption	Volcanic explosivity index (VEI)
Sheveluch	56.78°N, 161.58°E	02.18.1854	5
Askja	65.03°N, 16.75°W	03.29.1875	5
Krakatau	06.10°S, 105.42°E	08.26.1883	6
Tarawera	38.23°S, 176.51°E	06.10.1886	5
Santa Maria	14.76°N, 91.55°W	10.24.1902	6
Ksudach	51.83°N, 157.52°E	03.28.1907	5
Novarupta (Katmai)	58.27°N, 155.16°W	06.06.1912	6
Quizapu (Azul)	35.67°S, 70.77°W	04.10.1932	5
Bezymianny	56.07°N, 160.72°E	03.30.1956	5
Mount St. Helens[a]	46.20°N, 122.18°W	05.18.1980	5

a Main volcanic blast directed laterally, not vertically

in the same year as the eruption if the eruption takes place in the first half of the year (perhaps before the stratospheric vortex breaks down). Not all seasons were affected by these eruptions; low winter season temperatures show no apparent relationship to major eruptions, even following Krakatau, the effect of which is clearly visible in all the other seasons.

Extremely warm years are also apparent in the record. Some of these are clearly related to major El Nino events, particularly those years in which El Nino events recurred or persisted from the preceding year (e.g. 1878, 1900, 1926, 1941, 1958, 1973; see Quinn *et al.* (1978) for a chronology of major El Nino events] Interestingly, several of the largest explosive eruptions of the last 100 years have been followed by El Ninos which have tended to both minimise the (cooling) effect of the eruption and the (warming) effect of the El Nino. The remarkable decline in temperatures after the eruption of Katmai in 1912 is perhaps related to the absence of any major El Nino at the time, or in the immediate period thereafter. Further study of circulation anomalies following these events is currently underway.

Summary

Long-term temperature data from stations throughout the Northern Hemisphere indicate that most of the temperature increase of the last 130years took place between 1880 and 1930, particularly in the periods 1880–1900 and 1915–1930. Prior to 1880, temperatures appear to have increased from the 1850s to the 1870s, then declined. The lowest temperatures of the last 130 years during the early 1880s were probably accentuated by effects of the explosive eruption of Krakatau in 1883. After the 1930s, average temperatures decreased to levels similar to those of the 1920s. A slight upturn in temperatures has occurred over the last 10–15 years. The effects of major explosive volcanic eruptions and of exceptional El Nino events are seen as pronounced short-term cooling and warming events, respectively, superimposed on the low frequency temperature trends of the last 130 years. Data from China and the Northern Hemisphere land areas as a whole are highly correlated, particularly on time scales of the order of decades. This suggests that long-term proxy temperature data, from Chinese historical records, may be a useful indicator of temperature fluctuations over the Northern Hemisphere.

Acknowledgement. This work was supported by the U.S. Department of Energy, Contract DE–AC02–81– EV10739.

References

Bradley R S, Kelly P M, Jones P D, Diaz H F, Goodess C, M (1985) A climatic data bank for Northern Hemisphere land areas, 1851–1980. *Tech Rep TR* 017, Carbon Dioxide Research Division U S Dept Energy, Washington D C (in press)

Edmonds J A, Reilly J, Trabalka J R, Reichle D E (1984) An analysis of possible future atmospheric retention of fossil fuel CO_2. *Tech Rep TR* 013, Carbon Dioxide Research Division. U S Dept Energy, Washington, DC

Hensen J, John Son D, Lee P, Rind D, Russell G.(1981) *Science* 213; 957 – 966

Jones P D, Wigley T M L, Kelly P M (1982) *Mon Wea Rev* 110: 59 –70

Jones P D, Kelly P M (1983) *J Climato* 3: 243 –252

Keeling C D, Bacastow R B, Whorf T B (1982) in: Clark W. C. (ed) *Carbon Dioxide Rev* 1982. Oxford Univ Press, New York, pp 377 –385

Kelly P M, Sear C B (1984) *Nature* 311: 740 –743

Kelly P M, Jones P D, Sear C B, Cherry B S G, Tavakol R K (1982) *Mon Wea Rev* 110: 71 –82

Kelly P M, Jones P D, Wigley T M L, Bradley R S, Diaz H F, Goodess C M (1985) The extended Northern Hemisphere surface air temperature record: 1851 – 1984. In: *Extended Summaries 3rd Conf Climate Varia Symp Contemp Climate:* 1850–2100. Am Meteorol Soc Boston, Mass, pp 35 – 36

MacCracken M C, Luther F M (eds) (1985) *The Potential Climatic Effects of Increasing Carbon Dioxide.* U S Dept Energy, Washington D C (in press)

Manabe S, Wetherald R T (1980) *J Atmos Sci* 37: 99 –118

Mitchell J M Jr (1983) Empirical modeling of effects of solar variability, volcanic events and carbon dioxide on global-scale average temperature since A.D. 1880. in: McCormac B M (ed) *Weather and Climate Responses to Solar Variations.* Colorado Associated Univ Press, Boulder, pp 265 – 272

Quinn W H, Zopf D O, Short K S, Kuo Yang R T W (1978) *Fish Bull* 76: 663 – 678

Simkin T, Siebert L, McClelland L, Bridge D, Newhall C, Latter J H (1981) *Volcanoes of the world: a regional Directory, Gazetteer and Chronology of Volcanism, During the Last 10,000 years Hutchinson Ross,* stroudsburg, 232 pp

Stuiver M (1978) *Sicence* 199: 253 –258

Wigley T M L, Jones PD (1981) *Nature* 292: 205–298

Wigley T M L, Angell J, Jones P D (1985) Analyses of the atmospheric temperature record, Chap 4 in: MacCracken MC, Luther F M (eds) *Detecting the Climatic Effects of Increasing Carbon Dioxide.* US Dept Energy, Washington D C (in press)

Zhang Deer (1980) *Kexue Tongbao* 25: 497 – 500

Zhang Peiyuan, Gao-Fa Gong (1979) *Acta Meteoro Sin* 34: 238 – 247